Post-print version (generated on 14.09.2022)
This and other publications are available at:
http://www.acin.tuwien.ac.at/publikationen/ams/

Robotic precision 3D measurements in vibration-prone environments enabled by active six DoF sample-tracking

Daniel Wertjanz, Thomas Kern, Alexander Pechhacker, Ernst Csencsics and Georg Schitter

***Abstract*— This paper presents a six degree of freedom (DoF) active sample-tracking robotic 3D measurement system for inline applications. The integrated measurement platform (MP) of the state-of-the-art system is augmented by a compact and tailored in-plane tracking sensor system. Based on two position-sensitive devices and laser markers, relative motion between the 3D measuring tool on the MP and a sample surface is measured with sub-micrometer resolution. Applying a tailored high performance PID control architecture, a six DoF sample-tracking control bandwidth of about 450 Hz is achieved. In a translational in-plane DoF, vibrations with a dominant component at 66 Hz are reduced from 9.44µm rms by a factor of 10 to 931 nm rms. Experimental results successfully proof the system concept of robotic 3D measurements with sub-micrometer precision directly in a challenging vibration-prone environment.**

I. Introduction

Flexible, fast and precise inline measurements can improve industrial manufacturing processes by a 100 % quality control of the produced goods [1], [2]. The resulting continuous quality monitoring enables realtime optimization of production parameter settings to enhance the overall throughput as well as the production yield [3], [4]. Surface properties, such as topography and roughness, frequently serve as quality indicators, which is why precise 3D surface measurements are considered as a key technology in the semiconductor, automotive and consumer electronics sector [5]–[7].

To achieve the targeted flexible positioning of a 3D measurement tool (MT) at arbitrary measurement locations on a sample surface as well as to extend its measurement range, industrial robots can be employed [8], [9]. However, the limited positioning accuracy of modern industrial robots of several tens of micrometers [10], makes robots themselves not suitable for the demanded 3D surface measurements with single- or sub-micrometer resolution [11].

Similar to the positioning noise of a robot, environmental vibrations within an industrial production line may cause relative motion between the MT and the sample surface, resulting in corrupted 3D measurements due to motion blur [12]. Consequently, precision quality monitoring is typically conducted in vibration-free lab environments, usually impeding a 100% quality control of goods with structural sizes in the single-micrometer range without impairing the production throughput.

Recently, an active sample-tracking measurement system for precise robotic inline 3D surface inspection on freeforms has been reported [13], [14]. The feedback control-induced stiff link between the integrated MAGLEV measurement platform (MP) and the sample surface establishes lab-like conditions for the developed compact and lightweight scanning confocal chromatic sensor (SCCS) [15] mounted onto the MP. Currently, the system design includes three capacitive sensors to track a sample surface in the three out-of-plane degrees of freedom (DoFs), but is lacking appropriate in-plane tracking sensors for tracking the three remaining DoFs.

While there is a variety of high precision out-of-plane displacement sensors [16], fast, precise and compact in-plane sensors are hardly available. Multi-DoF speckle or image correlation-based micro-vision systems achieve spatial resolutions in the range of the several micrometer down to single-nanometer [17]–[20]. However, these camera-based measurement systems typically show rather low measurement rates of up to a few hundred Hertz [19], which is not expedient for the targeted high performance feedback-controlled sample-tracking application. To extend the current robotic measurement system's [13] sample-tracking capability from three to six DoFs, an in-plane measurement system based on position-sensitive devices (PSDs) may appear as a valid approach. Using laser-based markers, PSDs provide the required sub-micrometer resolution as well as a sufficient sensing range and bandwidth [21], [22].

The contribution of this paper is the successful demonstration of robotic 3D measurement with sub-micrometer precision within a challenging vibration-prone environment, enabled by a six DoF active sample-tracking approach.

After a presentation of the roboic 3D measurement system prototype in Section II, this paper focuses on i) the design of an integrated PSD-based in-plane tracking sensor system in Section III, ii) the design and implementation of the six DoF sample-tracking control (Section IV), and iii) the experimental tracking and 3D imaging performance evaluation in vibrational environment in Section V. Finally, Section VI concludes this paper.

II. Module for precise robotic 3D measurements

The concept of the active sample-tracking measurement system for precise robotic inline 3D surface inspection on freeforms is exemplarily shown for two DoFs in Fig.1. As can be seen, the measurement module acts as an endeffector of an industrial robot and is composed of a SCCS as precision 3D MT and a MAGLEV MP. Integrated tracking sensors measure the relative position of the SCCS to the sample surface

The authors are with the Christian Doppler Laboratory for Precision Engineering for Automated In-Line Metrology, Automation and Control Institute (ACIN), Technische Universität Wien, 1040 Vienna. Corresponding author: wertjanz@acin.tuwien.ac.at

Post-print version of the article: D. Wertjanz, T. Kern, A. Pechhacker, E. Csencsics, and G. Schitter, "Robotic precision 3D measurements in vibration-prone environments enabled by active six DoF sample-tracking," *Proceedings of the 2022 IEEE/ASME International Conference on Advanced Intelligent Mechatronics (AIM)*, 2022. DOI: 10.1109/AIM52237.2022.9863321
© 2022 IEEE. Personal use of this material is permitted. Permission from IEEE must be obtained for all other uses, in any current or future media, including reprinting/republishing this material for advertising or promotional purposes, creating new collective works, for resale or redistribution to servers or lists, or reuse of any copyrighted component of this work in other works.

Post-print version (generated on 14.09.2022)
This and other publications are available at:
http://www.acin.tuwien.ac.at/publikationen/ams/

(external MP position). By means of feedback control, a constant alignment of the SCCS relative to the sample surface is maintained, compensating also for robot pose-induced position uncertainties. In this way, the contactless stiff link between SCCS and sample surface actively compensates for relative motion and establishes lab-like conditions for the 3D MT.

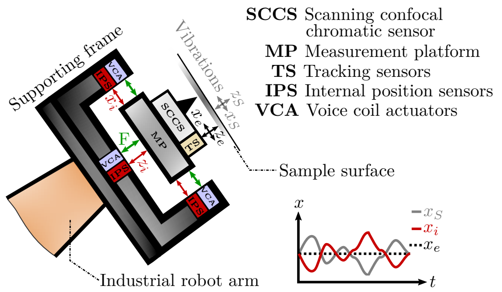

Fig. 1: Precise robotic inline 3D measurements on freeform surfaces. By maintaining a constant in-plane (x_e) and out-of-plane (z_e) position of the SCCS relative to the sample surface, disturbing vibrations (x_S and z_S) are actively compensated. On the bottom-right, the internal in-plane position signal x_i is exemplarily shown, compensating the sample vibrations x_S.

Considering the concept in Fig. 1, Fig. 2a shows the implemented robotic 3D measurement system prototype with the measurement module mounted to an industrial robot arm (KR 10 R900-2, KUKA AG, Augsburg, Germany). Figure 2b shows a zoomed image of the measurement module with the SCCS embedded in the MAGLEV MP. A balanced system design and the system's operability in arbitrary robot poses is achieved by employing eight identical voice coil actuators (VCAs) for the MP's quasi-zero-stiffness actuation. Six capacitive internal position sensors (IPSs) are integrated to measure the MP's position relative to the supporting frame (internal MP position), enabling a feedback-controlled stabilization of the MP in a free-floating position during a robot re-positioning. In order to achieve the targeted precision 3D measurements, the tailored, compact and lightweight SCCS has been developed as 3D MT [15], showing a lateral and axial resolution of down to 2.5 µm and 76 nm, respectively.

In its current state, the measurement module in Fig. 2b comprises three capacitive tracking sensors (TSs) to actively track a sample surface in the out-of-plane DoFs [13]. Due to their random characteristics, environmental vibration-induced disturbances can cause relative motion between the SCCS and the sample surface in all six DoFs [23]. Therefore, additional in-plane tracking sensors are required, which are compact and tailored for the operation on the MP. To enable the targeted high tracking performance of several hundred Hertz and sub-micrometer 3D measurements, the in-plane TS system is required to provide sub-micrometer resolution and a bandwidth exceeding 5 kHz.

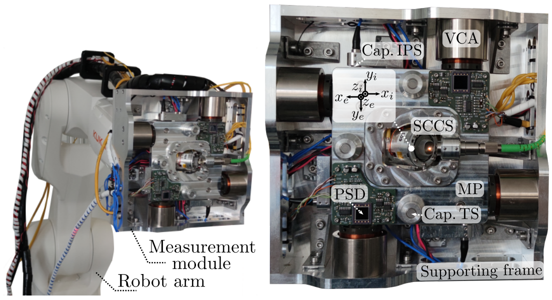

(a) Robotic 3D measurement system.
(b) 3D measurement module.

Fig. 2: Robotic 3D measurement system prototype. a) The measurement module is mounted to an industrial robot arm. b) The SCCS is embedded into the MP, which is actuated by VCAs. Integrated IPSs measure the MP position relative to the supporting frame. Three capacitive sensors and two PSDs are used to measure the relative motion between the SCCS and a sample surface.

III. In-plane Tracking Sensor System Design and Implementation

Given the limited number of compact in-plane displacement sensors available, a tailored and lightweight in-plane TS system based on two two-dimensional PSDs (S5991-01, Hamamatsu Photonics K.K., Hamamatsu, Japan) is designed. Each PSD provides four photo-currents, which are dependent on the light spot position of the used marker. Custom electronics are designed for signal conditioning, including transimpedance amplifiers as well as analog addition/subtraction circuits and are mounted on the bottom-left and top-right of the MP (see Fig. 2b). By setting the two lateral displacement-dependent photo-currents in relation to the sum current, the PSD characteristics can be linearized [24]. Therefore, besides the two lateral displacement-dependent signals, each PCB provides the according sum current-proportional signal. Two laser diodes (LDM650/1LJM, Roithner Lasertechnik GmbH, Vienna, Austria) are used as markers for the PSDs, providing a laser spots with a diameter of about 1 mm on each PSD.

As a stiff connection between the markers and the sample surface is necessary, the sample box in Fig. 3 is designed. It includes conductive targets for the three capacitive TSs, the laser diode-based markers for the in-plane TS system and a mounting for the sample surface to be precisely 3D imaged.

Optical disturbances, such as industrial lightning, can cause undesired noise within the targeted sensing bandwidth of the PSDs, which is why the modulation approach in Fig. 4 is pursued. Using the field programmable gate array (FPGA) of the rapid prototyping system (RPS) (MicroLabBox, dSPACE GmbH, Paderborn, Germany), a rectangular modulation signal $f_m = 50\,\text{kHz}$ is applied to the laser diode. The three modulated signals of each PSD, with u_x and u_y being the displacement-

Post-print version of the article: D. Wertjanz, T. Kern, A. Pechhacker, E. Csencsics, and G. Schitter, "Robotic precision 3D measurements in vibration-prone environments enabled by active six DoF sample-tracking," *Proceedings of the 2022 IEEE/ASME International Conference on Advanced Intelligent Mechatronics (AIM)*, 2022. DOI: 10.1109/AIM52237.2022.9863321
© 2022 IEEE. Personal use of this material is permitted. Permission from IEEE must be obtained for all other uses, in any current or future media, including reprinting/republishing this material for advertising or promotional purposes, creating new collective works, for resale or redistribution to servers or lists, or reuse of any copyrighted component of this work in other works.

Post-print version (generated on 14.09.2022)
This and other publications are available at:
http://www.acin.tuwien.ac.at/publikationen/ams/

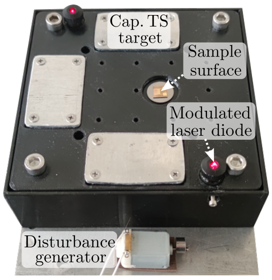

Fig. 3: Custom-made sample box. Conductive targets for the capacitive out-of-plane TSs and laser diodes as markers for the PSD-based in-plane TSs are rigidly to connected to a sample surface.

dependent voltage signals in x- and y-direction as well as u_s the signal proportional to the sum current, are fed to the ADC (10 MHz, 14 bit) of the RPS. The demodulation is performed on the FPGA by multiplying the three signals with the modulation source signal $\sin(2\pi f_m t)$. A subsequent digital 2nd order lowpass filter (**LP**) with a cut-off frequency of 10 kHz is the result of a trade-off between sufficient dynamic behavior and acceptable measurement noise. Subsequently, u'_x and u'_y are divided by u_s, linearizing the PSD's characteristics [24]. Finally, the resulting signals u''_x and u''_y are applied to a look-up table (**LUT**), which is used to compensate residual non-linearities and to calculate the two-dimensional position (x_{PSD} and y_{PSD}) of the laser spot on the PSD. This results in a positioning noise of about 200 nm rms for small lateral displacements, i.e. laser spots close to the PSD center, which meets the sub-micrometer precision requirement. For higher lateral displacements the position noise increases towards the single-micrometer level [22], which is, however, not relevant for the targeted compensation-based operation.

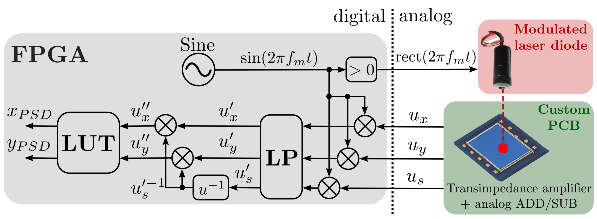

Fig. 4: Block diagram of the PSD-based in-plane tracking sensors. A laser diode is modulated with a frequency f_m and used as marker. Demodulation and subsequent digital lowpass filtering **LP** of the signals are performed and a look-up table **LUT** is used to calculate the measured lateral displacements x_{PSD} and y_{PSD}.

IV. System Analysis and Motion Control Design

With the additional TS system implemented and operable, the motion control of the integrated MAGLEV MP [13] is designed, requiring two individual control modes. First, the MP should be stabilized with respect to the supported frame when the robot is re-positioning and the TSs are not in range (stabilization mode). Second, with the TSs is range, the MP requires a high performance tracking control mode, which establishes the targeted contactless stiff link between the SCCS and the sample surface.

Figure 5 illustrates a schematic block diagram of the integrated MP's individual system components. Based on the actual MP positioning error $\mathbf{e}_\zeta$, the controller output $\mathbf{u}$ is calculated and transformed by a matrix $\mathbf{T}$ into the eight reference voltages $\mathbf{u_{a,r}}$ for the analog PI voltage-controlled current amplifiers $\mathbf{i_a}(\mathbf{u_{a,r}})$. The desired currents $\mathbf{i_a}$ are applied to the integrated VCAs [13], [14].

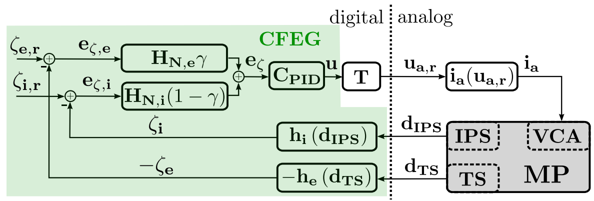

Fig. 5: Schematic block diagram of the integrated sample-tracking MP.

The measured distances $\mathbf{d_{IPS}}$ and $\mathbf{d_{TS}}$ by the integrated IPSs and TSs system need to be transformed into the actual internal and external MP position $\zeta_\mathbf{i}$ and $\zeta_\mathbf{e}$, respectively. Therefore, a set of trigonometric functions

$$\zeta_\mathbf{i} = \mathbf{h_i}(\mathbf{d_{IPS}}) \tag{1a}$$
$$\zeta_\mathbf{e} = \mathbf{h_e}(\mathbf{d_{TS}}) \tag{1b}$$

is applied and the two individual MP positions are obtained in six DoFs. Considering the two coordinate systems in Fig. 2b, the dynamics of the internal $\zeta_\mathbf{i}$ and external $\zeta_\mathbf{e}$ MP position differ solely in the sign, yielding

$$\dot{\zeta}_\mathbf{i} = -\dot{\zeta}_\mathbf{e} = -\mathbf{h_e}(\mathbf{d_{TS}}) \tag{2}$$

and enabling a cross-fading error gain (CFEG)-based transition scheme between the two individual control tasks [25].

As the system dynamics of the six DoF free-floating MP can only be identified in a feedback-controlled manner, six single-input single-output (SISO) floating mass model-based low-bandwidth proportional-integral-derivative (PID) controllers are designed and implemented. Low cross talk between the individual DoFs is obtained by the balanced MP design, justifying a SISO PID control architecture [13]. In Fig. 6, the identified dynamics and the subsequent controller design for the in-plane DoF x are exemplarily shown.

Considering the relation in (2) and the according implementation in Fig. 5, similar dynamics of the internal (G_i) and external dynamics (G_e) are measured for frequencies up to 900 Hz. Thus, the same PID control parameters can be applied for both control modes. The PID control parameters are synthesized and optimized in a loop-shaping approach to achieve the targeted high performance motion control [13]. A loop

Post-print version of the article: D. Wertjanz, T. Kern, A. Pechhacker, E. Csencsics, and G. Schitter, "Robotic precision 3D measurements in vibration-prone environments enabled by active six DoF sample-tracking," *Proceedings of the 2022 IEEE/ASME International Conference on Advanced Intelligent Mechatronics (AIM)*, 2022. DOI: 10.1109/AIM52237.2022.9863321
© 2022 IEEE. Personal use of this material is permitted. Permission from IEEE must be obtained for all other uses, in any current or future media, including reprinting/republishing this material for advertising or promotional purposes, creating new collective works, for resale or redistribution to servers or lists, or reuse of any copyrighted component of this work in other works.

Post-print version (generated on 14.09.2022)
This and other publications are available at:
http://www.acin.tuwien.ac.at/publikationen/ams/

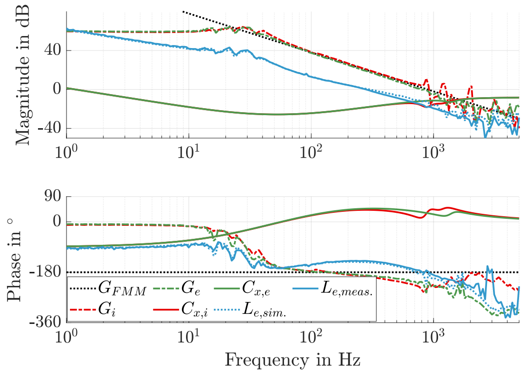

Fig. 6: Controller design for DoF x. The in- and external dynamics are in good accordance ($G_i \approx G_e$) and match the mathematical floating mass model G_{FMM}. The stabilization controller $C_{x,i}$ and tracking controller $C_{x,e}$ differ only by tailored notch filters at frequencies above 800 Hz.

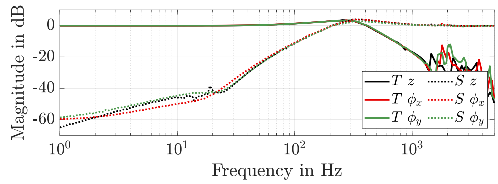

(a) Out-of-plane tracking control.

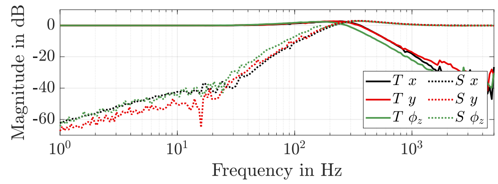

(b) In-plane tracking control.

Fig. 7: Complementary sensitivity T and sensitivity S of the implemented a) out-of-plane and b) in-plane tracking control. A -3 dB tracking control bandwidth of about 450 Hz and good disturbance rejection at low frequencies are achieved.

gain with a crossover frequency of $f_c = 300$ Hz is designed, yielding a robust gain and phase margin of 20 dB and 35°, respectively. The structural modes measured by the IPS and TS system of the MP slightly differ, which is most probably caused by the different sensor placement (see Fig. 2b). Therefore, individually tailored notch filters $\mathbf{H}_{\mathbf{N},\mathrm{k}}$, $k \in \{i, e\}$ are applied to ensure robustness.

As indicated in Fig. 6, the PID controllers $C_{x,i}$ (solid red) and $C_{x,e}$ (solid green) differ solely by the tailored and individually designed notch filters. Good accordance between the simulated $L_{e,sim.}$ and measured loop gain $L_{e,meas.}$ of the external MP position is achieved. A detailed discussion on the system modelling and controller design can be found in [13], [14]. With the designed and implemented CFEG-based control structure in Fig. 5, an efficient transition between the stabilization and tracking control is enabled [25].

In Fig. 7, the measured complementary sensitivity T and sensitivity function S of the six DoF tracking control (external position) are shown. A -3 dB tracking control bandwidth of about 450 Hz is achieved, with a good disturbance rejection in the lower frequency range.

V. Experimental Evaluation of Tracking and 3D Imaging Performance

The system's disturbance rejection capability to broadband vibrations in the out-of-plane DoFs is demonstrated in [13]. To generate and apply a six DoF disturbance to the horizontally mounted sample box, the eccentric motor in Fig. 3 is used. In the following, the tracking control performance the 3D imaging capability of the integrated robotic 3D measurement module in the vibration-prone environment is evaluated.

A. Tracking control performance

With the industrial robot positioning the 3D measurement module above the sample box such that all TSs are in mid-range, the disturbance generator is activated. For disabled tracking control, the tracking error, representing the sample vibration in each DoF, is shown in Fig. 8 (red). The measurement results reveal a vibrating sample surface with a dominant component at a frequency of 66 Hz and different magnitudes in the individual six DoFs. Focusing on the proposed in-plane TS tracking control (left column), the resulting disturbance in the translational in-plane DoF x is 9.44 µm rms. Repeating the measurement with enabled tracking control, the residual tracking errors for the attenuated disturbances are shown in black. The disturbance is reduced by a factor of 10 to a residual tracking error of about 931 nm rms, which corresponds to an attenuation of 20 dB and accords to the measured sensitivity S_x at the disturbance frequency of 66 Hz (see Fig. 7). For reasons of completeness, the out-of-plane tracking performance is shown in the right column of Fig. 8. Although in the translational out-of-plane DoF z a lower level vibration is induced, a disturbance attenuation factor of about 10 is maintained.

B. Precise 3D imaging in vibration-prone environment

Finally, the measurement module's 3D imaging performance in the vibrational environment is experimentally evaluated on a calibration standard (Nanuler Calibration Standard, Applied NanoStructures Inc., Mountain view, CA, USA), which is mounted in the center of the sample box (see Fig. 3). In Fig. 9, a microscope image of the structural surface under test is illustrated. Next to the L-structure with a height of 5.81 µm, also several surface defects are visible.

Initially, the disturbance generator as well as the tracking control are turned off and the SCCS performs a reference 3D measurement within a measurement time of $T_m = 10$ s. Considering the 3D measurement area in Fig. 9, the resulting 3D reference image in Fig. 10a clearly shows the structural

Post-print version of the article: D. Wertjanz, T. Kern, A. Pechhacker, E. Csencsics, and G. Schitter, "Robotic precision 3D measurements in vibration-prone environments enabled by active six DoF sample-tracking," *Proceedings of the 2022 IEEE/ASME International Conference on Advanced Intelligent Mechatronics (AIM)*, 2022. DOI: 10.1109/AIM52237.2022.9863321
© 2022 IEEE. Personal use of this material is permitted. Permission from IEEE must be obtained for all other uses, in any current or future media, including reprinting/republishing this material for advertising or promotional purposes, creating new collective works, for resale or redistribution to servers or lists, or reuse of any copyrighted component of this work in other works.

Post-print version (generated on 14.09.2022)
This and other publications are available at:
http://www.acin.tuwien.ac.at/publikationen/ams/

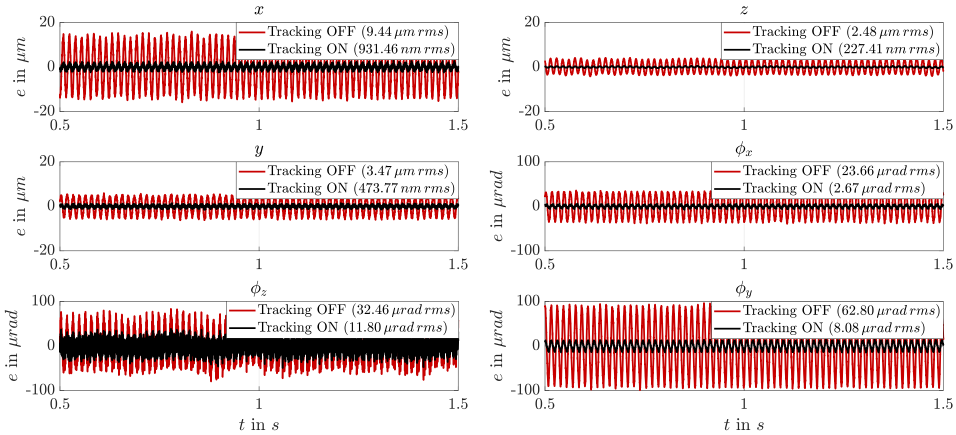

Fig. 8: Tracking error in each DoF for dis- and enabled tracking control. The vibrations (red) are successfully attenuated (black) by actively tracking the sample surface. Sub-micrometer precision is achieved in all translational DoFs.

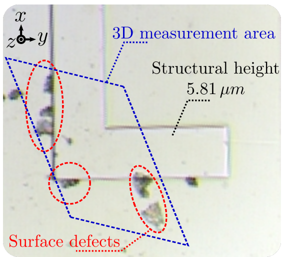

Fig. 9: Microscope image of the sample surface with a structural height of 5.81 µm. Several surface defects (red ellipses) are also visible within the 3D measurement area (blue).

sample surface of interest, including the aforementioned surface defects. The according cross section at $y = 250\,\mu\text{m}$ (dashed red) is analyzed in Fig. 10d (dotted black). As can be seen, a structural height of 5.89 µm is measured. Moreover, on the bottom-left for $x \in [30\,\mu\text{m}, 80\,\mu\text{m}]$, a surface defect is detected. Next, a 3D measurement is conducted with the vibrations applied to the sample surface but disabled tracking control. Figure 10b shows the corrupted measurement results due to the six DoF motion blur between the SCCS and the sample surface. Illustrated by the according cross section in Fig. 10d (red), the measured structural peak height of about 10 µm is not correct. Moreover, the surface defects in the interval of $x \in [30\,\mu\text{m}, 80\,\mu\text{m}]$ are also not visible. A repeated measurement with enabled tracking control to attenuate the disturbing vibrations yields the 3D measurement result in Fig.10c. Enabled by the feedback control-induced stiff link between the SCCS and the sample surface, the cross sections of the reference and vibration-compensated 3D measurement (solid black) in Fig. 10d are in good agreement. The measured structural height of about 5.89 µm corresponds to a measurement error of 80 nm. Additionally, the measurement result also resolves the small surface defect indicted on the bottom-left.

In summary, the proposed six DoF sample-tracking control establishes the targeted lab-like conditions for the SCCS by reducing the disturbing vibrations by a factor of 10, enabling robotic 3D measurements with sub-micrometer resolution within challenging vibration-prone environments.

VI. Conclusion

With an eye towards robot-based precision 3D measurement directly in the vibration-prone environment of an industrial production line, a six DoF sample-tracking MP with an integrated SCCS as 3D MT is proposed. By means of two PSDs mounted onto the MP and tailored laser diode-based markers, relative in-plane motion between the MP and the sample surface is measured on the sub-micrometer scale. A SISO PID control architecture is designed and implemented, achieving a six DoF tracking control bandwidth of about 450 Hz. Disturbing vibrations are applied to the sample surface in order to evaluate the system performance. Enabled by the feedback control-induced stiff link between SCCS and sample surface, experimental results demonstrate that a translational in-plane vibration with 9.44 µm rms and a dominant component at a frequency of 66 Hz is reduced by a factor of 10 to 931 nm rms. Demonstrated by 3D measurements with sub-micrometer precision within challenging vibration-prone environments, the targeted lab-like conditions for the integrated SCCS are successfully established.

Future work includes the integration of an automated robot repositioning in order to enable precision 3D meaurements on moving objects, such as conveyed goods in an industrial production line.

Acknowledgment

This project is partially funded by the Hochschuljubilaeumsfonds of the city of Vienna, Austria under the project number H-260744/2020. The financial support by the Christian Doppler

Post-print version of the article: D. Wertjanz, T. Kern, A. Pechhacker, E. Csencsics, and G. Schitter, "Robotic precision 3D measurements in vibration-prone environments enabled by active six DoF sample-tracking," *Proceedings of the 2022 IEEE/ASME International Conference on Advanced Intelligent Mechatronics (AIM)*, 2022. DOI: 10.1109/AIM52237.2022.9863321
© 2022 IEEE. Personal use of this material is permitted. Permission from IEEE must be obtained for all other uses, in any current or future media, including reprinting/republishing this material for advertising or promotional purposes, creating new collective works, for resale or redistribution to servers or lists, or reuse of any copyrighted component of this work in other works.

Post-print version (generated on 14.09.2022)
This and other publications are available at:
http://www.acin.tuwien.ac.at/publikationen/ams/

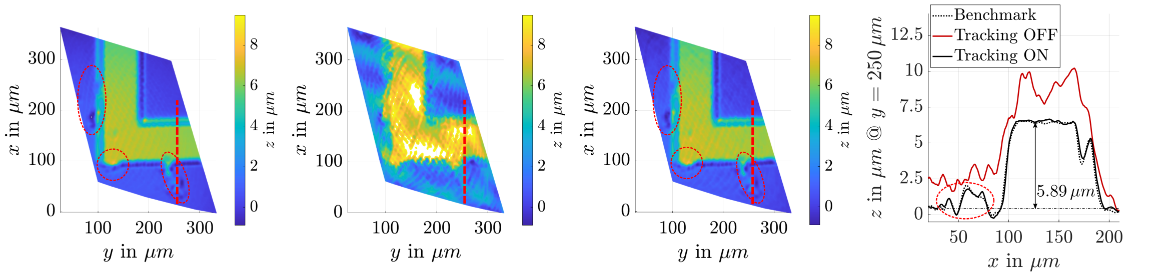

(a) Reference. (b) Tracking off. (c) Tracking on. (d) Cross section at $y = 250\,\mu\text{m}$.

Fig. 10: 3D imaging performance evaluation. a) shows the reference measurement with the structural surface clearly visible. The surface defects are inicated by the red ellipses. b) shows the 3D image for disabled tracking control in the vibrational environment with motion blur corrupting the measurement result. By enabling the active vibration compensation, the measured structural surface in c) is very similar as in the reference measurement. d) compares the cross sections (dashed red) in a)-c). Whereas the structural height is not precisely measured with disabled tracking control (red), the reference (dotted black) and vibration-compensated measurement (solid black) are in good accordance. A surface defect is indicated on the bottom-left.

Research Association, the Austrian Federal Ministry for Digital and Economic Affairs, and the National Foundation for Research, Technology and Development, as well as MICRO-EPSILON MESSTECHNIK GmbH & Co. KG and ATENSOR Engineering and Technology Systems GmbH is gratefully acknowledged.

References

[1] D. Imkamp, R. Schmitt, and J. Berthold, “Blick in die Zukunft der Fertigungsmesstechnik - Die VDI/VDE-GMA Roadmap Fertigungsmesstechnik 2020.” *Technisches Messen*, vol. 10, no. 79, 2012.

[2] R. Schmitt and F. Moenning, “Ensure success with inline-metrology,” in *XVIII IMEKO World Congress - Metrology for a Sustainable Development*, 2006.

[3] W. Gao, H. Haitjema, F. Fang, R. Leach, C. Cheung, E. Savio, and J. Linares, “On-machine and in-process surface metrology for precision manufacturing,” *CIRP Annals*, vol. 68, no. 2, pp. 843 – 866, 2019.

[4] M. Grasso and B. Colosimo, “Process defects and in situ monitoring methods in metal powder bed fusion: a review,” *Measurement Science and Technology*, vol. 28, p. 044005, 2017.

[5] H. Schwenke, U. Neuschaefer-Rube, T. Pfeifer, and H. Kunzmann, “Optical methods for dimensional metrology in production engineering,” *CIRP Annals*, vol. 51, no. 2, pp. 685–699, 2002.

[6] A. Yogeswaran and P. Payeur, “3d surface analysis for automated detection of deformations on automotive body panels,” in *New Advances in Vehicular Technology and Automotive Engineering*. IntechOpen, 2012.

[7] T.-F. Yao, A. Duenner, and M. Cullinan, “In-line dimensional metrology in nanomanufacturing systems enabled by a passive semiconductor wafer alignment mechanism,” *Journal of Micro- and Nano-Manufacturing*, vol. 5, no. 1, 2016.

[8] E. Savio, L. D. Chiffre, and R. Schmitt, “Metrology of freeform shaped parts,” *CIRP Annals*, vol. 56, no. 2, pp. 810 – 835, 2007.

[9] J. Rejc, J. Cinkelj, and M. Munih, “Dimensional measurements of a gray-iron object using a robot and a laser displacement sensor,” *Robotics and Computer-Integrated Manufacturing*, vol. 25, no. 2, pp. 155–167, 2009.

[10] U. Schneider, M. Drust, M. Ansaloni, C. Lehmann, M. Pellicciari, F. Leali, J. Gunnink, and A. Verl, “Improving robotic machining accuracy through experimental error investigation and modular compensation,” *The International Journal of Advanced Manufacturing Technology*, vol. 85, pp. 1–13, 2014.

[11] E. Csencsics, M. Thier, S. Ito, and G. Schitter, “Supplemental peak filters for advanced disturbance rejection on a high precision endeffector for robot-based inline metrology,” *IEEE/ASME Transactions on Mechatronics (Early Access)*, 2021.

[12] R. Saathof, M. Thier, R. Hainisch, and G. Schitter, “Integrated system and control design of a one dof nano-metrology platform,” *Mechatronics*, vol. 47, pp. 88 – 96, 2017.

[13] D. Wertjanz, T. Kern, E. Csencsics, and G. Schitter, “Bringing the lab to the fab: Robot-based inline measurement system for precise 3D surface inspection in vibrational environments,” *IEEE Transactions on Industrial Electronics*, 2022, accepted.

[14] D. Wertjanz, E. Csencsics, and G. Schitter, “Three-dof vibration compensation platform for robot-based precision inline measurements on free-form surfaces,” *IEEE Transactions on Industrial Electronics*, vol. 69, no. 1, pp. 613–621, 2022.

[15] D. Wertjanz, T. Kern, E. Csencsics, G. Stadler, and G. Schitter, “Compact scanning confocal chromatic sensor enabling precision 3-d measurements,” *Appl. Opt.*, vol. 60, no. 25, pp. 7511–7517, 2021.

[16] C. P. Keferstein and M. Marxer, *Fertigungsmesstechnik*. Wiesbaden: Springer Verlag, 2015.

[17] Z.-H. Chen and P. S. Huang, “A vision-based method for planar position measurement,” *Measurement Science and Technology*, vol. 27, no. 12, p. 125018, 2016.

[18] V. Guelpa, P. Sandoz, M. A. Vergara, C. Clévy, N. Le Fort-Piat, and G. J. Laurent, “2d visual micro-position measurement based on intertwined twin-scale patterns,” *Sensors and Actuators A: Physical*, vol. 248, pp. 272–280, 2016.

[19] H. Li, B. Zhu, Z. Chen, and X. Zhang, “Realtime in-plane displacements tracking of the precision positioning stage based on computer micro-vision,” *Mechanical Systems and Signal Processing*, vol. 124, pp. 111–123, 2019.

[20] E. Csencsics, “Integrated compensation-based laser sensor system for in-plane and out-of-plane target tracking,” *Appl. Opt.*, vol. 59, no. 20, pp. 6138–6147, 2020.

[21] K. Liu, W. Wang, Y. Yu, X. Hou, Y. Liu, W. Chen, X. Wang, J. Lu, and Z. Ni, “Graphene-based infrared position-sensitive detector for precise measurements and high-speed trajectory tracking,” *Nano Letters*, vol. 19, no. 11, pp. 8132–8137, 2019.

[22] H. W. Yoo, D. Brunner, T. Thurner, and G. Schitter, “Mems test bench and its uncertainty analysis for evaluation of mems mirrors,” *IFAC-PapersOnLine*, vol. 52, no. 15, pp. 49–54, 2019, 8th IFAC Symposium on Mechatronic Systems MECHATRONICS 2019.

[23] C. G. Gordon, *Generic Vibration Criteria for Vibration-Sensitive Equipment*, Colin Gordon & Associates, 1999.

[24] H. P. K.K., *Two-dimensional PSD - S5990/S5991 series*, Hamamatsu, Japan, 2020, retrieved on 2022/02/11.

[25] D. Wertjanz, E. Csencsics, and G. Schitter, “An efficient control transition scheme between stabilization and tracking task of a maglev platform enabling active vibration compensation,” in *2020 IEEE/ASME International Conference on Advanced Intelligent Mechatronics (AIM)*, 2020, pp. 1943–1948.

Post-print version of the article: D. Wertjanz, T. Kern, A. Pechhacker, E. Csencsics, and G. Schitter, “Robotic precision 3D measurements in vibration-prone environments enabled by active six DoF sample-tracking,” *Proceedings of the 2022 IEEE/ASME International Conference on Advanced Intelligent Mechatronics (AIM)*, 2022. DOI: 10.1109/AIM52237.2022.9863321

© 2022 IEEE. Personal use of this material is permitted. Permission from IEEE must be obtained for all other uses, in any current or future media, including reprinting/republishing this material for advertising or promotional purposes, creating new collective works, for resale or redistribution to servers or lists, or reuse of any copyrighted component of this work in other works.